university of groningen / faculty of science and engineering / mathematics and applied mathematics

Clustering-based model reduction of a network of nonlinear oscillators

Bachelor's Project Applied Mathematics

July 10, 2019

Student: A.J. Raven

First supervisor: dr. ir. B. Besselink

Second supervisor: dr. A.E. Sterk

Abstract

In this thesis we study the reduction of networks of oscillators. Specifically, the oscillators are given by neuron models characterized through nonlinear differential equations. We consider modular networks, which consist of modules of nodes with directed connections to the subsequent module, essentially forming a cycle. Given the network structure we can consider a model reduction by means of clustering. We are interested in preserving some characteristic dynamical behaviour of the network when applying this model reduction. In particular, we want to preserve the stability region for traveling wave solutions, which only occurs for certain coupling strengths of the modules and the cycle structure. We find that clustering does well in approximating this stability region compared to other more trivial simplifications of the network. We find that the accuracy of the approximation depends on the similarity of the solutions of the nodes which are clustered.

Keywords: FitzHugh-Nagumo oscillator, modular networks, clustering-based model reduction, MatCont, bistability

Contents

Chapter 1

Introduction

Models are used everywhere to replicate real life phenomena. We use models, among other things, to predict the weather, to simulate the launch of a rocket or to determine population growth. There are a multitude of fields where models are prevalent. In this thesis we are interested in a biological model called the FitzHugh-Nagumo model. The FitzHugh-Nagumo (FHN) model is a simplification of the Hodgkin-Huxley model which replicates the activation and deactivation of a spiking neuron. This model was created by Richard FitzHugh in 1961 [3]. The FHN model is a type of biological neuron model which falls into the category of electrical input-output membrane voltage models. The aim is to replicate the operations of a nervous system. This can help better the understanding of how the brain functions and communicates with the body. Therefore, it would be necessary to look at networks of such models to be able to represent a network of neurons. The simulation of a network of neurons will result in having to solve a large system of Ordinary Differential Equations (ODE). Solving this numerically can quickly lead to long computation times. Hence, it would be useful to look into a reduction of the model in order to simplify the problem and lower the computation time. In this thesis we will look into applying a clustering-based model reduction on a modular network of FHN oscillators. We are interested in seeing whether this simplification of the model will carry over some of the qualitative behavior of the original system.

Research has been done on networks of FHN oscillators. In a paper by Steur et al., they investigate the dynamics of modular networks of coupled nonlinear oscillators. They employ the FHN model to describe the dynamics of the oscillators in the nodes of the network and are able to confirm the co-existence of synchronization and traveling waves. Furthermore, they ran numerical analysis to determine the prevalence of traveling wave solutions when changing the number of nodes in each module of the network [7]. In another paper written by Steur et al., they find further results for a network with a ring structure, using the same dynamics for the nodes, of the prevalence of traveling wave solutions when varying the number of nodes and the coupling strength [9]. There has also been progress in the use of clustering-based model reduction on many types of

networks. Cheng has applied a clustering-based model reduction on second-order networks and directed networks, among others, in hopes of preserving the network structure [2].

Existing works only consider a clustering-based model reduction of linear networks. However, linear networks do not show the same complex behaviour as observed in the network of Steur. Therefore, in this thesis I will apply a clustering-based model reduction on nonlinear networks with the aim of preserving the occurrence of traveling wave solutions. Investigating the clustering-based model reduction of a network of FHN oscillators will give insight on how well such a simplification can approximate the original system as well as observe which dynamical properties are still present in the model reduction. Some ubiquitous properties can be examined and argued whether they can be generalized to different networks or for different dynamics of the oscillators in the nodes. This will contribute to the research of conserving dynamical properties for a clustering-based model reduction of a network, as there is a lack of research on this specific topic.

In Chapter 2 we will introduce the model used for the rest of the thesis. This includes a description of the FHN oscillator as well as the network structure. In Chapter 3 we will consider a model reduction by clustering the system. The process of deriving the clustering-based model reduction of our system will be detailed in this chapter. In Chapter 4 we will go over some background information needed to understand how the stability of a traveling wave solution is characterized and also how to determine when there is a change of stability for this solution. In Chapter 5 we will present all of the results. This will mainly be the stability regions for the different networks we consider. In Chapter 6 we will recap what we have done and draw some conclusions. Suggestions will be given for future research on our topic.

Chapter 2

Modelling

In this thesis we will consider a network of coupled nonlinear oscillators described in the work of Steur [7]. For this reason we start by introducing the dynamics of the oscillator and the structure of the network.

2.1 FitzHugh-Nagumo Oscillator

The system of FitzHugh-Nagumo (FHN) oscillators considered in the paper by Steur are described by

$$\begin{cases} \dot{y}_j = y_j - \gamma y_j^3 - z_j + u_j, \\ \dot{z}_j = \alpha(y_j - \beta z_j), \end{cases} \tag{2.1}$$

where α, β, γ are parameters with the chosen values

$$\alpha = \frac{8}{100}, \beta = \frac{8}{10}, \gamma = \frac{1}{3}. \tag{2.2}$$

The state variables y_j and z_j represent the membrane potential and recovery potential of a spiking neuron, respectively. A typical solution for a single FHN oscillator is illustrated in Figure 2.1. The index j labels the individual nodes. The input u_j represents the coupling of the network which will be determined in the next section. It will be convenient for derivations in a later chapter to rewrite the model in a compact form. First we write the differential equations as a single equation. To this end, define the vector

$$x_j = \begin{bmatrix} y_j \\ z_j \end{bmatrix}.$$

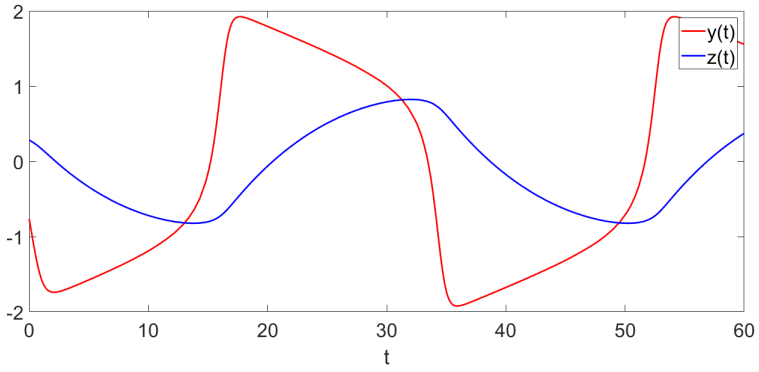

Figure 2.1: Solution of a single FHN oscillator (2.1), with the parameter values given in (2.2) and the input $u_j(t) = 0$ for all t.

Then, the pair of differential equations in (2.1) can be rewritten to

$$\begin{cases} \dot{x}_j = \begin{bmatrix} 1 & -1 \\ \alpha & -\alpha\beta \end{bmatrix} x_j + \begin{bmatrix} 1 \\ 0 \end{bmatrix} (u_j - \gamma y_j^3), \\ \\ y_j = \begin{bmatrix} 1 & 0 \end{bmatrix} x_j. \end{cases} \tag{2.3}$$

For convenience we define the matrices

$$A = \begin{bmatrix} 1 & -1 \\ \alpha & -\alpha\beta \end{bmatrix}, \; B = \begin{bmatrix} 1 \\ 0 \end{bmatrix}, \; C = \begin{bmatrix} 1 & 0 \end{bmatrix},$$

and also the function $\phi : \mathbb{R} \to \mathbb{R}$, defined by $\phi(y_j) = y_j^3$. Consider a network of $n \in \mathbb{N}$ oscillators. Let

$$x = \begin{bmatrix} x_1 \\ x_2 \\ \vdots \\ x_n \end{bmatrix}, \; y = \begin{bmatrix} y_1 \\ y_2 \\ \vdots \\ y_n \end{bmatrix}, \; u = \begin{bmatrix} u_1 \\ u_2 \\ \vdots \\ u_n \end{bmatrix}, \; \Phi = \begin{bmatrix} \phi(y_1) \\ \phi(y_2) \\ \vdots \\ \phi(y_n) \end{bmatrix}.$$

Note that $x \in \mathbb{R}^{2n}$, while $y, u, \Phi \in \mathbb{R}^n$. A collection of systems shown in (2.3) is then described by

$$\begin{cases} \dot{x} = (I_n \otimes A)x + (I_n \otimes B)(u - \gamma\Phi(y)), \\ y = (I_n \otimes C)x, \end{cases} \tag{2.4}$$

where $I_n \in \mathbb{R}^{n \times n}$ is the identity matrix. The notation $\otimes$ refers to the Kronecker product. For a matrix $V \in \mathbb{R}^{m \times n}$ and $W \in \mathbb{R}^{p \times q}$ the Kronecker product is

defined as

$$V \otimes W = \begin{bmatrix} v_{11}W & v_{12}W & \dots & v_{1n}W \\ v_{21}W & v_{22}W & \dots & v_{2n}W \\ \vdots & \vdots & \ddots & \vdots \\ v_{m1}W & v_{m2}W & \dots & v_{mn}W \end{bmatrix},$$

where the matrix $V \otimes W \in \mathbb{R}^{mp \times nq}$ and $v_{ij} = [V]_{i,j}$, i.e. the element of matrix V in the i-th row and j-th column. In essence, what the Kronecker product accomplishes in system (2.4) is duplicating the dynamics of a single oscillator given in (2.3) to all n oscillators. Hence, all oscillators in the collection of systems will have the same dynamics, only differing in their coupling u_j.

We were able to write a collection of FHN oscillators in a compact form, which will be useful in deriving a so-called clustered version of the network in the next chapter. What follows is to describe the structure of the network and determine what form the input u has.

2.2 Network

In this section we will describe the structure of the network presented in the paper by Steur. The goal is to derive the form of the input u.

In graph theory a network is a graph in which nodes and/or edges can have attributes assigned to them. A graph is composed of nodes/vertices and edges. Typically a graph is denoted by G, the nodes by V and edges by E. We can think of the FHN oscillators as nodes and the connection between them, or rather transmission of information between oscillators, as edges. Recall that all of the oscillators in the network have the same dynamics, i.e. we have identical nodes. Furthermore, an edge can be directed or undirected, meaning one-way flow or two-way flow of information respectively. A directed edge is represented by an arrow, indicating the direction in which the information is transmitted. An undirected edge is represented by a line between nodes. The i-th node is denoted by v_i. The network we consider is illustrated in Figure 2.2.

In Figure 2.2 we see several groups of nodes called modules. Furthermore, in these modules all nodes are connected with one another, making this a highly structured network. There is also one node in each module connected to a node in the next module forming a cycle/ring. The structure of the network can be represented in what is known as the graph Laplacian $L(G)$. To define the graph Laplacian, we first introduce the so-called adjacency matrix of G.

$$[A(G)]_{i,j} = \begin{cases} 1 \text{ if there is an edge from } v_i \text{ to } v_j, \\ 0 \text{ otherwise.} \end{cases}$$

Note that the nodes are not connected to themselves, so the diagonal of the adjacency matrix consists of 0's. Next we still need to introduce the so-called degree matrix of G, which is a diagonal matrix whose main diagonal represents the degree of the nodes. The degree of a node corresponds to the number of

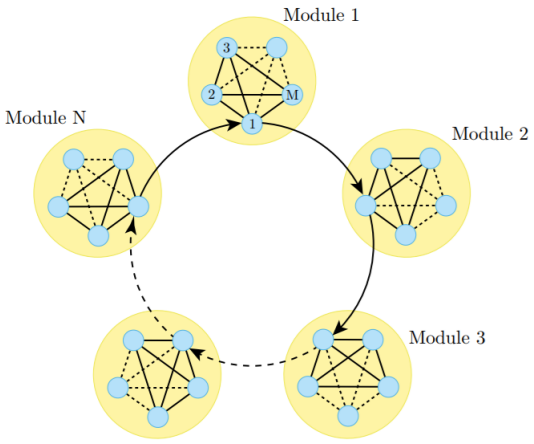

Figure 2.2: Modular network structure considered in Steur's paper [7].

neighbours it has. However, for a directed graph there is a distinction between in-degree and out-degree. These correspond to the number of incoming and outgoing edges, respectively. To define the degree matrix we need to declare which degree we will use. In this thesis we will only consider balanced directed graphs, that is, for every node the in-degree and out-degree are equal [5]. Therefore, we can define the degree matrix by

$$[\Delta(G)]_{i,i} = \sum_{j=1}^{n} [A(G)]_{i,j},$$

i.e. by summing the elements in a row of the adjacency matrix. Now that the adjacency matrix and degree matrix have been introduced we can define the graph Laplacian.

$$L(G) = \Delta(G) - A(G).$$

For the remainder of this section we will derive the graph Laplacian for the network in Figure 2.2. To this end, it will be useful to first number the nodes of the network. The network as described in Figure 2.2 is made out of N modules, each consisting of M nodes. Following the illustration, the first M nodes are the nodes found in module 1. Then from $M+1$ to $2M$ are the nodes in module 2, etc. For convenience, we will start by giving the graph Laplacian for a single module in the network. The graph Laplacian for a singular module is given by

$$\Gamma_m = \begin{bmatrix} M-1 & -1 & \dots & -1 \\ -1 & M-1 & \ddots & -1 \\ \vdots & \ddots & \ddots & \vdots \\ -1 & -1 & \dots & M-1 \end{bmatrix}.$$

Here $\Gamma_m \in \mathbb{R}^{M\times M}$, M being the number of nodes in the module. All the nodes in the module are connected with one another, meaning the adjacency matrix is made up of all 1's except for the main diagonal which is all 0's. Consequently. the degree matrix has $M-1$ as its entry on the main diagonal. However, the network illustrated in Figure 2.2 consists of N modules. Therefore, the interconnection described in Γ_m needs to be "duplicated" to all the other modules to be able to represent the modular structure of the network. This can be done in a similar fashion as was done when describing the dynamics of the oscillators in (2.4). That is, by using the Kronecker product. So the interconnection of all the modules in the network can be represented by $I_N \otimes \Gamma_m$.

It only remains to represent the cycle in the network, that being the directed connection of a single node in each module, see Figure 2.2. We need to again determine the graph Laplacian. Here we only consider the nodes which are constituents of the aforementioned cycle. This means, we are considering the following N nodes v_1, v_{M+1},..., $v_{(N-1)M+1}$. The graph Laplacian of the cycle is given by

$$\Gamma_r = \begin{bmatrix} 1 & -1 & 0 & \dots & 0 \\ 0 & 1 & -1 & \ddots & \vdots \\ \vdots & \ddots & \ddots & \ddots & 0 \\ 0 & \dots & 0 & 1 & -1 \\ -1 & 0 & \dots & 0 & 1 \end{bmatrix},$$

with $\Gamma_r \in \mathbb{R}^{N\times N}$. The cycle has a clockwise flow meaning that the adjacency matrix is given by $[A]_{i,i+1} = 1$ and the rest of the entries are 0's. Therefore, the degree matrix is simply the identity matrix. This results in the graph Laplacian Γ_r as shown above. However, this interconnection describes the cycle of N nodes next to each other, but the cycle in our network is for the nodes v_1, v_{M+1},..., $v_{(N-1)M+1}$. Therefore, we need to "spread out" the interconnection. This can again be done with the help of the Kronecker product. The interconnection of the cycle in the network is then given by $\Gamma_r \otimes B$. Here the matrix B is given by

$$B = \begin{bmatrix} 1 & 0 & \dots & 0 \\ 0 & 0 & \dots & 0 \\ \vdots & \vdots & \ddots & \vdots \\ 0 & 0 & \dots & 0 \end{bmatrix},$$

where $B \in \mathbb{R}^{M\times M}$. The Kronecker product $\Gamma_r \otimes B$ is essentially putting $M-1$ zeroes in between each entry of Γ_r, thus spreading the interconnection to the correct position.

In a later chapter we want to do bifurcation analysis on this network. In particular we want to research the dependence of the module structure and cycle structure. Therefore, it will be necessary to introduce the parameters $\sigma \in \mathbb{R}_{\geq 0}$ and $\mu \in \mathbb{R}_{\geq 0}$, which are the inter-modular and intra-modular coupling strengths, respectively. In other words σ corresponds to the interconnection strength of the module structure and μ corresponds to the interconnection strength of the cycle

structure. The complete interconnection of the network considered in Figure 2.2 is therefore described by the coupling matrix

$$\Gamma(\sigma, \mu) = \sigma\Gamma_r \otimes B + I_N \otimes \mu\Gamma_m. \tag{2.5}$$

Hence, we have derived the coupling matrix which describes the interconnections of the network. We are now able to describe the input u introduced in the model of the system in the previous section. The input is given by

$$u = -\Gamma(\sigma, \mu)y, \tag{2.6}$$

where u and y are in vector form. From the form of the coupling matrix given in (2.5) we can see that the system has a so-called diffusive coupling. That is, the coupling is defined by the weighted difference of the output signals of the system [8]. This characteristic in combination with other assumptions allows for certain properties of the system to be proved, such as boundedness of the solution or ensuring synchronization of the system.

2.3 Problem Statement

The network introduced has modules in which all nodes are connected with one another. These nodes are clumped together only having one node directing information to another module. It might seem reasonable then to consider a model reduction in which we consider the clumped nodes as a single entity. This can be done via clustering, which will be discussed in the next chapter. An interesting aspect to look into is how well the model reduction via clustering carries over the dynamical behaviour of the original network. In particular, the network of FHN oscillators given by (2.4) and (2.6) has an interesting characteristic called bistability. This means that, for some fixed values of the inter- and intramodular strengths, it produces two stable solution, those being synchronization and traveling wave solutions. Synchronization is characterized by oscillator solutions that are equal with common phase, and traveling wave solutions by oscillator solutions that are equal, but with different phase. Synchronization solutions are present for any value of the coupling strengths σ and μ. However, traveling wave solutions only appear for some values of the coupling strengths. We want to be able to derive a stability region depicting where the traveling wave solutions occur depending on the coupling strengths, see Figure 2.3 for an example.

The main goal of this thesis is to be able to obtain the stability region for traveling wave solutions pertaining to different network structures and compare them to the stability region of the clustered system. We hope to find that clustering a network is a good approximation in terms of conserving the stability region for traveling waves solutions. In the next chapter we will define what stability means for a periodic solution, which can be used to define the stability for traveling wave solutions.

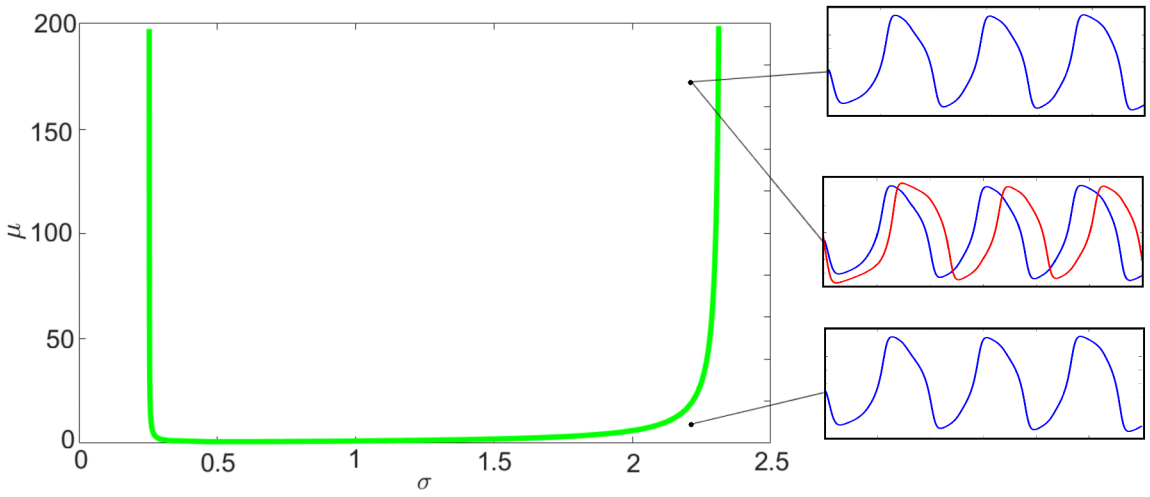

Figure 2.3: Bistability graph for Steur's network consisting of 5 modules, each containing 5 nodes ($N = 5$, $M = 5$), with the parameter values given in (2.2). Inside the curve is a region where both stable solutions occur when changing the initial conditions of the system. This is then the stability region for traveling wave solutions.

Chapter 3

Model Reduction by Clustering

This chapter will focus on deriving a reduced model of the network introduced in the previous chapter. One choice for a model reduction on a network is to simplify it by reducing the number of nodes. In particular, this can be done by partitioning the network into several non-overlapping clusters, in which a group of nodes is regarded as a single node [2]. Usually a cluster will contain a group of nodes with a similar function in the network in hopes of preserving some dynamical behaviour of the original network, in this case the stability region for traveling wave solutions. Such a clustering-based model reduction can be done by introducing a cluster matrix and applying a Petrov-Galerkin projection, thus reducing the dimension of the system. In this chapter we will focus on applying a clustering-based model reduction on the network described by (2.4).

3.1 Cluster Matrix

To apply the model reduction we first have to define the cluster matrix. We first consider a clustering $\pi = \{C_1, C_2, ..., C_k\}$ of the graph G for a network of n oscillators. The cluster matrix of the partition π is defined by

$$[P(\pi)]_{i,j} = \begin{cases} 1 \text{ if } v_i \in C_j, \\ 0 \text{ otherwise,} \end{cases} \tag{3.1}$$

with $P \in \mathbb{R}^{n \times k}$ [6]. In order to give a more intuitive description of the matrix P, we will derive the cluster matrix for a module of the network as described in Figure 2.2. The ordering of the nodes is as defined in the previous chapter. If we take a look at the structure of the network one might think to cluster the whole module. However, we have to keep in mind that one of the nodes is directing information to the subsequent module. Hence, to preserve the structure of the network it might be better to cluster all the nodes excluding the one connected

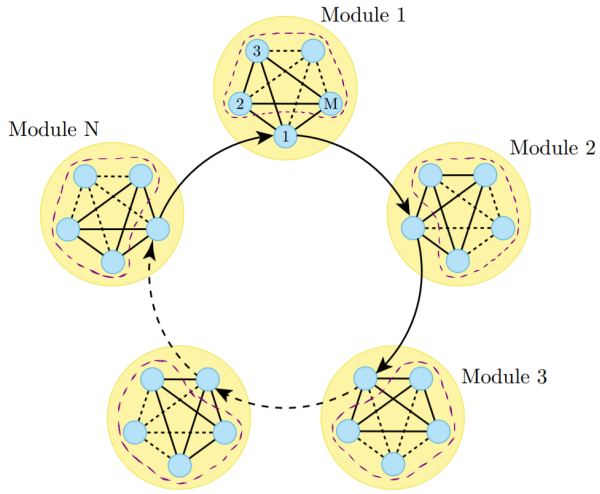

Figure 3.1: Clustering of Steur's network. All the nodes in a module except for one pertaining to the ring structure are clustered together, as indicated by the purple dashed lines.

to the next module. This yields a cluster matrix of the form

$$\hat{P} = \begin{bmatrix} 1 & 0 \\ 0 & 1 \\ \vdots & \vdots \\ 0 & 1 \end{bmatrix}, \tag{3.2}$$

where $\hat{P} \in \mathbb{R}^{M\times 2}$, M being the number of nodes in a module. In this case, node v_1 is left alone while the remaining nodes v_2,v_3,...,v_M are clumped together, i.e. we have the clustering $C_1 = \{v_1\}$, $C_2 = \{v_2, v_3, ..., v_M\}$. This clustering is depicted in Figure 3.1 for all of the modules in the network. This is then generalized to the rest of the modules by using the Kronecker product on (3.2). The cluster matrix for the whole network is then given by

$$P = I_N \otimes \hat{P}. \tag{3.3}$$

Similarly, one can consider to cluster the whole module as was first considered. In this case, the $\hat{P}$ matrix is an $M \times 1$ vector of 1's. In the next section we will derive a clustering-based reduced-order approximation of our network.

3.2 Clustered Network Dynamics

At the end of the previous chapter we derived an expression for u given by (2.6). Recall from (2.4) that $y = (I_n \otimes C)x$. The expressions for y and u can

be substituted into the differential equation in (2.4) resulting in

$$\dot{x} = (I_n \otimes A)x + (I_n \otimes B)(-\Gamma(I_n \otimes C)x - \gamma\Phi((I_n \otimes C)x)). \tag{3.4}$$

This equation can be further simplified by applying an identity of the Kronecker product called the mixed-product property. The mixed-product property gives the following identity for matrices A,B,C,D

$$(A \otimes B)(C \otimes D) = AB \otimes CD, \tag{3.5}$$

given that the matrix products AB and CD are possible. Note that $\Gamma = \Gamma \otimes 1$. Hence, applying (3.5) to (3.4) leads to

$$\dot{x} = (I_n \otimes A)x - (\Gamma \otimes BC)x - \gamma(I_n \otimes B)\Phi((I_n \otimes C)x). \tag{3.6}$$

Describing the system in this way allows for a more systematic approach to a clustering-based model reduction. This will be done by approximating the state vector x in the following way

$$x \approx (P \otimes I_2)\xi, \tag{3.7}$$

where $P \in \mathbb{R}^{n\times k}$ and $\xi \in \mathbb{R}^{2k}$. Here P represents the cluster matrix and ξ represents the reduced-order state vector of the clustered network. The integer k corresponds to the number of partitions made when clustering the network. Substituting the approximation of x shown in (3.7) into (3.6) results in

$$\begin{aligned}(P \otimes I_2)\dot{\xi} = (I_n \otimes A)(P \otimes I_2)\xi - (\Gamma \otimes BC)(P \otimes I_2)\xi \\ - \gamma(I_n \otimes B)\Phi((I_n \otimes C)(P \otimes I_2)\xi).\end{aligned}$$

This expression can be simplified by applying the mixed-product property introduced in (3.5). This leads to

$$(P \otimes I_2)\dot{\xi} = (P \otimes A)\xi - (\Gamma P \otimes BC)\xi - \gamma(I_n \otimes B)\Phi((P \otimes C)\xi). \tag{3.8}$$

Recall that generally the cluster matrix P is not square. Therefore, to later be able to invert the term in front of $\dot{\xi}$ it is better to have a square matrix. One option which will be utilized is to pre-multiply (3.8) by $(P^T \otimes I_2)$ which results in

$$\begin{aligned}(P^T \otimes I_2)(P \otimes I_2)\dot{\xi} = (P^T \otimes I_2)(P \otimes A)\xi - (P^T \otimes I_2)(\Gamma P \otimes BC)\xi \\ - \gamma(P^T \otimes I_2)(I_n \otimes B)\Phi((P \otimes C)\xi).\end{aligned} \tag{3.9}$$

The mixed-product property (3.5) can again be applied to produce

$$(P^T P \otimes I_2)\dot{\xi} = (P^T P \otimes A)\xi - (P^T \Gamma P \otimes BC)\xi - \gamma(P^T \otimes B)\Phi((P \otimes C)\xi). \tag{3.10}$$

We want to extract the cluster matrix P from the function Φ in (3.10). Notice that $P = P \otimes 1$, which allows us to write $P \otimes C = (P \otimes 1)(I_k \otimes C)$. We can define the vector $\hat{y} = (I_k \otimes C)\xi$ and show how to separate the cluster matrix from $\hat{y}$ with the help of Lemma 3.2.1.

Lemma 3.2.1. *Let $\hat{y}$ be the vector as defined before and P be the cluster matrix. Then the following holds*

$$\Phi(P\hat{y}) = P\hat{\Phi}(\hat{y}), \text{ where } \hat{\Phi}(\hat{y}) = \begin{bmatrix} \phi(\hat{y}_1) \\ \phi(\hat{y}_2) \\ \vdots \\ \phi(\hat{y}_k) \end{bmatrix}.$$

Proof. To prove this we start by introducing some new notation. First let $A \in \mathbb{R}^{m\times n}$ be an arbitrary matrix. Then the operator $A\hat{}3$ is defined by

$$A\hat{}3 = \begin{bmatrix} (a_{11})^3 & (a_{12})^3 & \dots & (a_{1n})^3 \\ (a_{21})^3 & (a_{22})^3 & \dots & (a_{2n})^3 \\ \vdots & \vdots & \ddots & \vdots \\ (a_{m1})^3 & (a_{m2})^3 & \dots & (a_{mn})^3 \end{bmatrix},$$

i.e. cubing the terms of the matrix. This allows us to write $\Phi(P\hat{y}) = (P\hat{y})\hat{}3$. Next we note that the cluster matrix can be given in the block diagonal form

$$P = \begin{bmatrix} \mathbb{1}_{C_1} & 0 & \dots & 0 \\ 0 & \mathbb{1}_{C_2} & \dots & 0 \\ \vdots & \vdots & \ddots & \vdots \\ 0 & 0 & \dots & \mathbb{1}_{C_k} \end{bmatrix},$$

where $\mathbb{1}_{C_i}$ is a column vector consisting of 1's. This form can always be achieved by reordering the nodes in the graph. We then have

$$\begin{aligned} \Phi(P\hat{y}) = (P\hat{y})\hat{}3 &= \left(\begin{bmatrix} \mathbb{1}_{C_1} & 0 & \dots & 0 \\ 0 & \mathbb{1}_{C_2} & \dots & 0 \\ \vdots & \vdots & \ddots & \vdots \\ 0 & 0 & \dots & \mathbb{1}_{C_k} \end{bmatrix} \begin{bmatrix} \hat{y}_1 \\ \hat{y}_2 \\ \vdots \\ \hat{y}_k \end{bmatrix} \right)\hat{}3 \\ &= \begin{bmatrix} \hat{y}_1\mathbb{1}_{C_1} & 0 & \dots & 0 \\ 0 & \hat{y}_2\mathbb{1}_{C_2} & \dots & 0 \\ \vdots & \vdots & \ddots & \vdots \\ 0 & 0 & \dots & \hat{y}_k\mathbb{1}_{C_k} \end{bmatrix}\hat{}3 \\ &= \begin{bmatrix} \phi(\hat{y}_1)\mathbb{1}_{C_1} & 0 & \dots & 0 \\ 0 & \phi(\hat{y}_2)\mathbb{1}_{C_2} & \dots & 0 \\ \vdots & \vdots & \ddots & \vdots \\ 0 & 0 & \dots & \phi(\hat{y}_k)\mathbb{1}_{C_k} \end{bmatrix} \\ &= \begin{bmatrix} \mathbb{1}_{C_1} & 0 & \dots & 0 \\ 0 & \mathbb{1}_{C_2} & \dots & 0 \\ \vdots & \vdots & \ddots & \vdots \\ 0 & 0 & \dots & \mathbb{1}_{C_k} \end{bmatrix} \begin{bmatrix} \phi(\hat{y}_1) \\ \phi(\hat{y}_2) \\ \vdots \\ \phi(\hat{y}_k) \end{bmatrix} = P\Phi(\hat{y}) \end{aligned}$$

□

Since $P \otimes C = (P \otimes 1)(I_k \otimes C)$ we can rewrite the third term on the right hand side of (3.10) to

$$\begin{aligned}\gamma(P^T \otimes B)\Phi((P \otimes C)\xi) &= \gamma((P^T \otimes B)(P \otimes 1)\hat{\Phi}((I_k \otimes C)\xi) \\ &= \gamma(P^T P \otimes B)\hat{\Phi}((I_k \otimes C)\xi).\end{aligned} \tag{3.11}$$

The first equality of (3.11) follows from Lemma 3.2.1. We can now plug (3.11) into (3.10) resulting in

$$\begin{aligned}(P^T P \otimes I_2)\dot{\xi} = (P^T P \otimes A)\xi &- (P^T \Gamma P \otimes BC)\xi \\ &- \gamma(P^T P \otimes B)\hat{\Phi}((I_k \otimes C)\xi).\end{aligned}$$

In order to cancel out the term in front of $\dot{\xi}$ we want to pre-multiply the equation above by $(P^T P \otimes I_2)^{-1}$ to produce

$$\begin{aligned}(P^T P \otimes I_2)^{-1}(P^T P \otimes I_2)\dot{\xi} = (P^T P \otimes I_2)^{-1}&(P^T P \otimes A)\xi \\ &- (P^T P \otimes I_2)^{-1}(P^T \Gamma P \otimes BC)\xi \\ &- \gamma(P^T P \otimes I_2)^{-1}(P^T P \otimes B)\hat{\Phi}((I_k \otimes C)\xi).\end{aligned} \tag{3.12}$$

Note that

$$\begin{aligned}(P^T P \otimes A) &= (P^T P \otimes I_2)(I_k \otimes A), \\ (P^T P \otimes B) &= (P^T P \otimes I_2)(I_k \otimes B).\end{aligned}$$

This allows the inverse terms to cancel out from the first and third terms on the right hand side of (3.12). Furthermore, we make use of the following property of the Kronecker product. Let A and B be arbitrary invertible matrices. Then,

$$(A \otimes B)^{-1} = A^{-1} \otimes B^{-1}.$$

Hence, the second term on the right hand side of (3.12) can be rewritten to

$$\begin{aligned}(P^T P \otimes I_2)^{-1}(P^T \Gamma P \otimes BC)\xi &= ((P^T P)^{-1} \otimes (I_2)^{-1})(P^T \Gamma P \otimes BC)\xi \\ &= ((P^T P)^{-1} P^T \Gamma P \otimes BC)\xi\end{aligned}$$

Thus, the approximation is simplified to

$$\dot{\xi} = (I_k \otimes A)\xi - (\hat{\Gamma} \otimes BC)\xi - \gamma(I_k \otimes B)\hat{\Phi}((I_k \otimes C)\xi), \tag{3.13}$$

where

$$\hat{\Gamma} = (P^T P)^{-1} P^T \Gamma P.$$

Notice how the dynamics for the clustered system in (3.13) has the exact same form as the dynamics of the original system in (3.6). This means that the clustered system can be seen as a smaller network of oscillators. The key distinction

between the networks is in the coupling, where the coupling matrix $\hat{\Gamma}$ of the clustered network is transformed by the cluster matrix P. What this transformation is essentially doing is taking the average of the interconnection, as described in the coupling matrix Γ, of the clustered nodes. To elaborate on this, we mean that the i-th rows and separately the i-th columns, where i corresponds to the nodes being clustered, are summed up and then all entries in the resulting row and column are divided by the number of nodes being clustered. This means that in our case the clustering-based model reduction boils down to reducing the network size and transforming the coupling matrix by taking the mean of the interconnection of the clustered nodes.

Now that we have derived the dynamics for the clustering-based model reduction we are interested in studying the stability of a certain type of solution this network produces, called the traveling wave solution. This is the topic of the next chapter.

Chapter 4

Stability of the Traveling Wave Solution

The topic of this chapter will be to look into the stability of solutions occurring in a network of FHN oscillators. The one of interest is the traveling wave solution, which occurs for certain fixed values of the coupling strengths. We want to be able to determine the stability region for traveling wave solutions when varying the coupling strengths of the network. Hence, we will start by looking at the characteristics of the solution of the FHN oscillator and find a way to determine the stability of its solutions. In the second section we give a little background information on what happens at a bifurcation point.

4.1 Limit Cycles

We will start by considering a continuous-time dynamical system with the following dynamics

$$\dot{x} = f(x),\ x \in \mathbb{R}^n. \tag{4.1}$$

A solution $x(t)$ of system (4.1) is called periodic or closed, if there exists some time $T > 0$ such that

$$x(t) = x(t + T).$$

The minimal time T with this property is called the period. The path which a solution follows is called the trajectory, and a cycle is the trajectory of a periodic solution. With this we can present a definition for a limit cycle.

Definition 4.1.1 ([4, p. 10])**.** A cycle of a continuous-time dynamical system, in a neighbourhood where no other cycles occur, is called a limit cycle.

We want to define what a stable cycle is, which would extend to a limit cycle. To this end, we will first define what stability means for a fixed point of a discrete-time dynamical system and then relate this to a periodic solution by introducing the Poincaré Map.

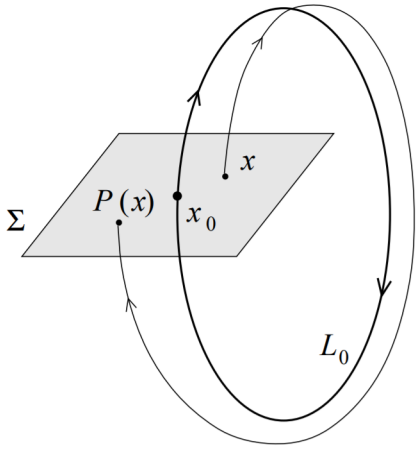

Figure 4.1: Poincare map for a given cycle [4, p. 26].

Theorem 4.1.2 ([4, p. 17])**.** *Consider a discrete-time dynamical system described by*

$$x \mapsto f(x), \quad x \in \mathbb{R}^n.$$

We call x^0 a fixed point if it satisfies

$$f(x^0) = x^0.$$

Let $A = \frac{\partial f}{\partial x}(x^0)$ denote the Jacobian matrix of f evaluated at the fixed point. Then the fixed point is stable if all eigenvalues $\mu_1, \mu_2 ..., \mu_n$ of A satisfy $|\mu_i| < 1$.

The eigenvalues of a fixed point are often called multipliers. We will now look into defining the Poincaré Map. Suppose we have a cycle, denoted by L_0, of system (4.1). Let x_0 be a point on this cycle and introduce the cross-section Σ to the cycle at the point x_0, see Figure 4.1. Any trajectories near the cycle L_0 with a starting point $x \in \Sigma$ will return to the cross-section Σ at some point $\tilde{x} \in \Sigma$. This allows for the construction of the following map.

Definition 4.1.3 ([4, pp. 26–27])**.** The map $P : \Sigma \to \Sigma$, defined by

$$x \mapsto \tilde{x} = P(x),$$

is called the Poincaré Map associated with the cycle L_0.

It is possible to apply a coordinate change, after which the origin is the fixed point of the map, i.e. $P(0) = 0$. It then follows that the cycle is stable if the multipliers $\mu_1, \mu_2, ..., \mu_{n-1}$ of the Jacobian of P are such that $|\mu_i| < 1$ for $i = 1, 2, ..., n-1$. This follows from Theorem 4.1.2. However, it remains to be shown how this relates to the continuous-time dynamical system in (4.1).

Let $x(t)$ be a periodic solution of system (4.1). Consider a neighbouring trajectory given by

$$\tilde{x}(t) = x(t) + \epsilon(t), \tag{4.2}$$

for ϵ small. Taking this neighbouring trajectory as a solution to the dynamical system described in (4.1) leads to

$$\dot{\tilde{x}}(t) = f(\tilde{x}(t)) = f(x(t) + \epsilon(t)).$$

However, taking the time derivative of (4.2) also yields

$$\dot{\tilde{x}}(t) = \dot{x}(t) + \dot{\epsilon}(t) = f(x(t)) + \dot{\epsilon}(t).$$

Therefore, we have that

$$f(x(t)) + \dot{\epsilon}(t) = f(x(t) + \epsilon(t)). \tag{4.3}$$

If we take the Taylor series of the function $f(x(t) + \epsilon(t))$ at the point $x(t)$ we find

$$f(x(t) + \epsilon(t)) \approx f(x(t)) + \frac{\partial f}{\partial x}(x(t))\epsilon(t) + \mathcal{O}(\epsilon^2), \tag{4.4}$$

where $\frac{\partial f}{\partial x}(x(t))$ denotes the Jacobian of the function f. By substituting (4.4) into (4.3) and subtracting $f(x(t))$ from both sides we end up with

$$\dot{\epsilon}(t) = \frac{\partial f}{\partial x}(x(t))\epsilon(t). \tag{4.5}$$

Recall that $x(t)$ is assumed to be a periodic solution, such that $\frac{\partial f}{\partial x}(x(t+T)) = \frac{\partial f}{\partial x}(x(t))$. Hence, system (4.5) is a periodic system with period T and is called the variational equation [4]. The time-dependent matrix $M(t)$ is called the fundamental matrix solution of (4.1) if it satisfies

$$\dot{M}(t) = \frac{\partial f}{\partial x}(x(t))M(t), \quad M(0) = I_n. \tag{4.6}$$

Any solution of (4.5) satisfies

$$\epsilon(T) = M(T)\epsilon(0), \tag{4.7}$$

where $M(T)$ is called the monodromy matrix. We now give a theorem related to the monodromy matrix.

Theorem 4.1.4 ([4, p. 29])**.** *The monodromy matrix M(T) has eigenvalues*

$$1, \mu_1, \mu_2, ..., \mu_{n-1},$$

where μ_i correspond to the multipliers of the Jacobian of the Poincaré Map.

Notice that one of the multipliers is always equal to 1. This follows from the fact that taking a variation in the direction of the cycle will again result in a cycle. The eigenvalues of the monodromy matrix are often called the Floquet multipliers [10].

So, we have that a cycle corresponding to a periodic solution of system (4.1) is stable if all of its Floquet multipliers are located inside the unit circle. Since the traveling wave solution is a periodic solution of the network of FHN oscillators we can determine its stability with the theory covered in this chapter.

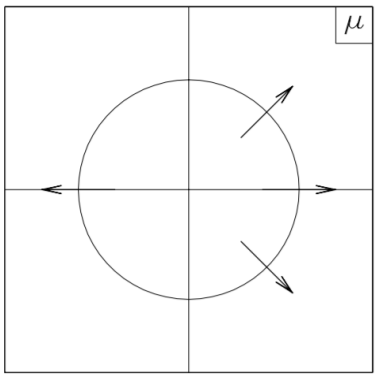

Figure 4.2: Loss of stability [10].

4.2 Bifurcation Theory

In this section we briefly go over the bifurcations associated with a loss of stability. We will then mention which bifurcation is of importance when determining the stability region for traveling wave solutions.

A bifurcation occurs when a change to the parameter values of a system causes a qualitative or topological change to its behaviour [1]. We are interested in what is called a local bifurcation, where varying the parameter causes a change in stability of an equilibrium or fixed point. Local bifurcations of a discrete-time dynamical system correspond to a fixed point having a Floquet multiplier with modulus 1. We can relate a periodic solution of a continuous-time dynamical system to such a fixed point with the Poincaré map introduced in the previous section. There are three ways in which a periodic solution can lose its stability.

1. A Floquet multiplier may leave the unit circle at the point (1,0).
2. A Floquet multiplier may leave the unit circle at the point (-1,0).
3. A pair of Floquet multipliers may leave the unit circle.

Case 1 leads to a so-called steady bifurcation, case 2 leads to a flip or period doubling bifurcation and case 3 leads to a Hopf or Neimark-Sacker bifurcation [10]. We are mainly interested in the Neimark-Sacker bifurcation, as it turns out to correspond to the point at which there is a stability change in the traveling wave solution of the network of oscillators we are considering. If a Neimark-Sacker bifurcation occurs in a Poincaré Map of a limit cycle, then a unique two-dimensional invariant torus bifurcates from the cycle.

Now that we know how to use the Floquet multipliers to determine the stability of traveling wave solutions, we can numerically determine its stability region. This will be done in the next chapter.

Chapter 5

Results

The main objective is to be able to determine the stability region for traveling wave solutions occurring in a network of FHN oscillators and compare it to the stability region of a reduced network obtained by clustering-based model reduction. In the first section we start by explaining how we go about finding the stability region. To derive the stability region we make use of a numerical continuation package in MATLAB. In this section we will briefly go over the steps of finding the stability region. In the second section we look at the stability regions for different network structures and discuss them.

5.1 Finding the Stability Region

The procedure of finding the stability region for traveling wave solutions can be characterized by the following steps

1. Find initial conditions which produce a traveling wave solution and determine its stable limit cycle.

2. Find the Neimark-Sacker bifurcation by varying the value of one of the coupling strengths.

3. Find the stability region by varying the values of both coupling strengths.

For the first step I implemented a script in MATLAB to solve the nonlinear ODEs of the FHN oscillators. This was done using the ode45 function. This function is based off of an explicit Runge-Kutta (4,5) formula. As input it takes the function handle, time span and initial condition of the ODE you want to solve. Then, it outputs a column vector t which corresponds to the time span and a solution array y. By using random initial conditions and running the script multiple times we notice that the oscillator solutions sometimes converge to a single wave or in other times there is a phase difference between the oscillator solutions, see Figure 5.1. These two solutions correspond to a synchronized and a traveling wave solution, respectively.

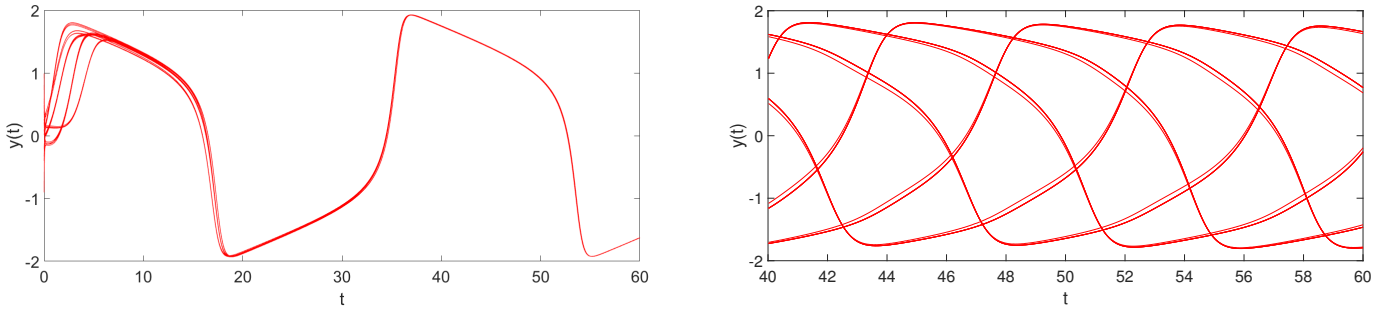

Figure 5.1: The two stable solutions which occur for a network of FHN oscillators ($N = 5$, $M = 5$). The parameter values are indicated in (2.2), with the coupling strengths $\sigma = 1$, $\mu = 6$. On the left is the synchronized solution and on the right is the traveling wave solution.

We are interested in determining the stability region of the traveling wave solution when varying the coupling strengths σ and μ. To this end, we need to do bifurcation analysis on the system. To help with this we will employ the use of a MATLAB package called MatCont. This package is a numerical continuation package for bifurcation analysis of dynamical systems. MatCont is capable of continuing equilibria and limit cycles of systems of ODEs. Since we know that the FHN oscillator produces a periodic solution, we will need to look into the continuation of a limit cycle. The initial conditions found earlier which produce a traveling wave solution can be plugged into MatCont. The numerical continuation package has access to all standard ODE solvers supplied by MATLAB to solve the system of ODEs. One of which, is the ode45 we utilized in our script. The choice of ODE solver depends on the accuracy one wants for their solution. In this case we will use ode45 to remain consistent. By plotting two different solutions of the system against each other we can depict a trajectory in the phase portrait in which we can identify a stable limit cycle, see Figure 5.2.

In the second step we want to investigate this stable limit cycle. We can choose to vary one of the parameters of the system. The parameters of interest are the coupling strengths. Since we have a traveling wave solution we know that we are in its stability region. We now want to vary one of the coupling strengths to determine when we leave this region. We choose to vary the parameter σ, which corresponds to the inter-modular coupling strength. MatCont is then able to compute the Floquet multipliers of the system, which are used to determine when the system undergoes a bifurcation. MatCont has the option to track different types of bifurcations. From the previous chapter we know to track the Neimark-Sacker bifurcation to determine when there is a change in stability of the traveling wave solution. MatCont is able to determine the point at which a Floquet multiplier leaves the unit circle, which corresponds to the value of σ at which there is a loss of stability of the traveling wave solution.

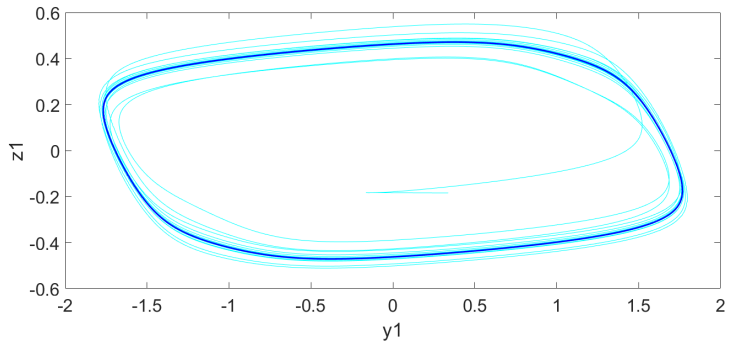

Figure 5.2: A limit cycle for an FHN oscillator. This is for a network of size $N = 5$, $M = 5$. The parameter values are indicated in (2.2), and the coupling strengths are $\sigma = 1$, $\mu = 6$. The inner dark blue closed trajectory highlights the stable limit cycle.

The final step is to do a continuation of this point and vary two parameters, these being both coupling strengths. By doing a continuation of this point we can determine the curve of Neimark-Sacker bifurcations which correspond to a stability change of the system. The inside of the curve corresponds to the stability region of the traveling wave solution of the network. The previous two steps are depicted in Figure 5.3. In the next section we will present the stability region for different networks and compare them to their model reductions.

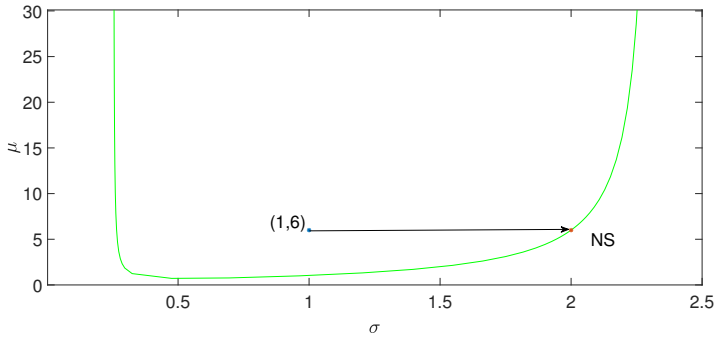

Figure 5.3: The procedure of determining the stability region. In this example we start at the point $(\sigma, \mu) = (1, 6)$ and increase σ till we find the Neimark-Sacker (NS) bifurcation to the right. Then we vary both σ and μ and obtain the curve.

5.2 Stability Regions

5.2.1 Steur's Network

The first network we consider is Steur's network, depicted in Figure 2.2. We want to determine its stability region for traveling wave solutions and see how well a model reduction of the network preserves this stability region. We consider the following cases for a model reduction of the network.

1. Clustering-based model reduction by clustering all but one of the nodes in each module.

2. Reduce the network size by lowering the number of nodes in each module to two.

3. Clustering-based model reduction by clustering all of the nodes in each module.

The first model reduction we consider was discussed in Chapter 3.1. The argument for choosing this clustering was to somehow preserve the ring structure of the network. Another argument can be made by taking a closer look at the traveling wave solution. What happens is that each wave with a phase difference is comprised of the solutions for the oscillators in a module. So, the number of waves with a phase difference corresponds to the number of modules in the network. Furthermore, we observe that the oscillators in a module almost synchronize. However, they do not completely synchronize since we can see two distinct waves, see Figure 5.4. The upper wave is comprised of $M-1$ oscillator solutions and the lower wave is comprised of a single oscillator solution. It turns out that this single oscillator solution corresponds to the node in the module which constitutes to the ring structure of the network. Hence, clustering the almost synchronized $M-1$ oscillators should yield a good approximation of the system.

For the model reduction in case 2 we reduce the network size. Since clustering reduces the number of nodes which need to be computed it would be interesting to compare this with a simplification where we consider a smaller network. Since we chose to cluster the network in such a way that there are only two nodes remaining in each module, we consider a simplified network consisting of two nodes per module.

Lastly, we look at another model reduction which might yield better results than reducing the network size. That is, we consider another clustering of the network where we now cluster all of the nodes in each module. This is a further simplification of the previous clustering. However, clustering the whole module will result in a loss of the intra-modular coupling μ from the coupling matrix. Consequently, we can only vary the inter-modular coupling strength σ.

Following the steps in the previous section we can determine the stability region for traveling wave solutions occurring in Steur's Network and its model reduction, see Figure 5.5 and Figure 5.6.

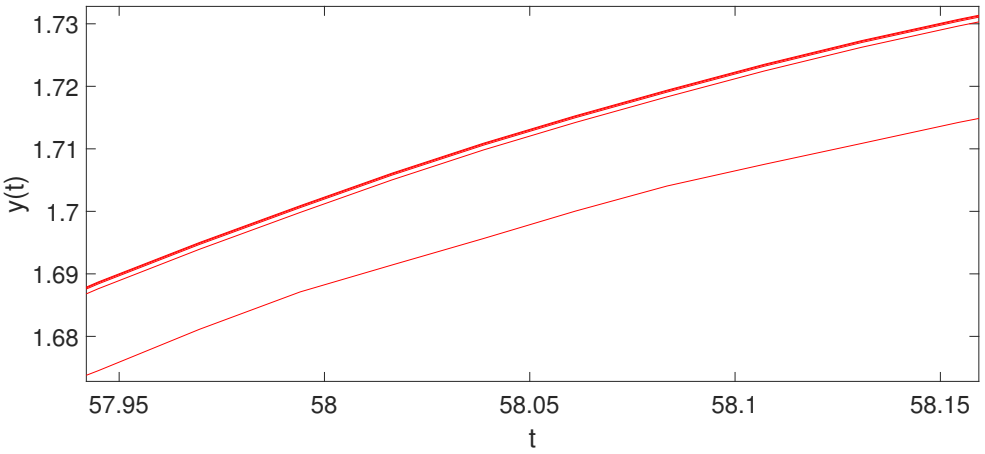

Figure 5.4: A closer look at the traveling wave solution in Figure 5.1.

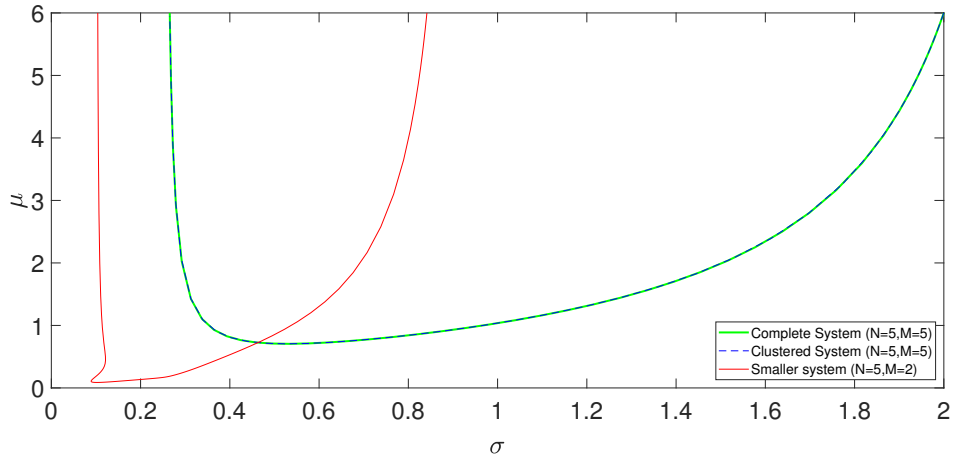

Figure 5.5: Stability regions for Steur's network and for its model reductions considered in cases 1 and 3. The parameter values are given in (2.2).

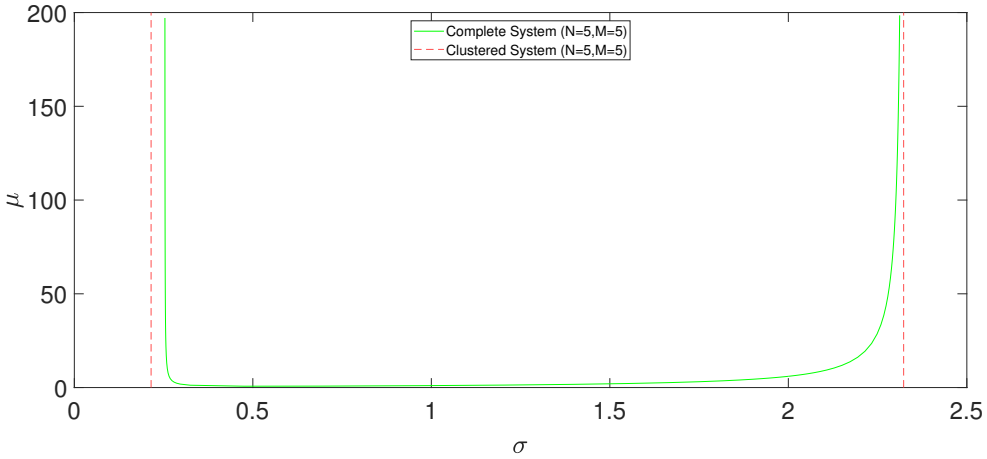

Figure 5.6: Stability regions for Steur's network and for its model reduction considered in case 2. The parameter values are given in (2.2).

In Figure 5.5 the blue and green dashed curves correspond to the stability region for traveling wave solutions of the original network and for the model reduction considered in case 1, respectively. The red curve corresponds to the stability region of the model reduction in case 2. In Figure 5.6 we compare the original network with the model reduction in case 2. Recall that we could only vary one of the coupling strengths for this model reduction. This results in only being able to find two points at which there is a stability change of the traveling wave solution. Depicting these points as vertical lines we obtain the red dashed lines illustrated in Figure 5.6. The stability region for the original network is again given by the green curve.

We will now discuss the results found for Steur's network. In case 1 we found that the resulting curve overlaps with the curve of the original network. This is not a common occurrence. So the fact that the clustered system has the same stability region is quite remarkable. This is possibly due to the highly interconnected modules, i.e. the fact that all nodes in a module are interconnected with one another. Another reason as to why case 1 is so good at preserving the stability region was shown with the help of Figure 5.4. What happens when we cluster the $M-1$ almost synchronized nodes in each module is that we are essentially taking the average of the oscillator solutions pertaining to the cluster. This means that a cluster will yield a better approximation of the original network when the clustered nodes have similar oscillator solutions.

Moving onto case 2, we found that reducing the network size is worse at preserving the stability region than clustering the network. There is an overlap between the stability region of the original network and the model reduction in case 2, but it really does not compare to model reductions by means of clustering. Why exactly is there a difference? As stated before the cluster is

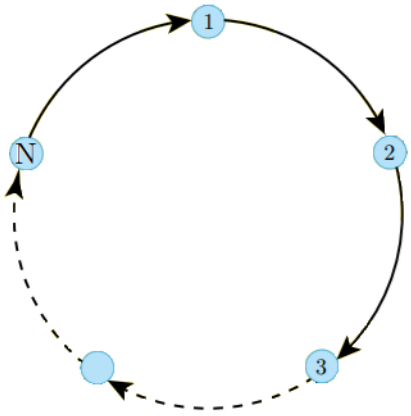

Figure 5.7: Ring Network consisting of N nodes.

essentially taking the average of the solutions of the nodes involved. This also takes into account the interconnection term given in (2.6). This means that the clustered system carries over some of the structure of the larger network. However, in case 2 we are simply considering a smaller network which has a different structure than the original network.

Lastly, we look at case 3. Here we found that the modular structure breaks down, leaving only the coupling strength corresponding to the ring structure. This meant that we could only find two points at which there is a stability change and plot them as vertical lines. However, these two lines still encompass the stability region of the original network. Particularly, the right vertical line looks like a vertical asymptote for the curve. We would have expected it to be a good approximation since we have observed that all the oscillator solutions in a module are relatively closely grouped together, see Figure 5.4. It does not preserve the stability region as well as the model reduction in case 1 because the modular structure breaks down.

What we want to do in the next section is look at different network structures and observe how well clustering can approximate the stability region of these networks.

5.2.2 Ring Network

In this section we will consider a different network structure than the one presented in Steur's paper. One network structure we can consider is a simple ring structure. An illustration of this network is shown in Figure 5.7. Since this network does not have any modules we can only assign a coupling strength to the ring structure, denoted by σ. A cluster we can consider is to group two adjacent nodes, e.g. grouping v_1 with v_2, v_3 with v_4, etc. With this type of clustering we will need an even number of nodes in the network. Therefore, we

	Left boundary	**Right boundary**
Original network (N=24)	0.001694	11.107
Clustered network (N=24)	0	5.5555
Smaller network (N=12)	0	2.7775

Table 5.1: The points at which there is a change in stability of the traveling wave solution for the ring structure. The parameter values are given in (2.2).

chose to investigate a ring with 24 nodes, i.e. $N = 24$. The clustering matrix is given by

$$P = I_{\frac{N}{2}} \otimes \begin{bmatrix} 1 \\ 1 \end{bmatrix}.$$

Since we have clusters of two nodes we will have $\frac{N}{2}$ clusters in total, hence why we "duplicate" the vector $\frac{N}{2}$ times using the Kronecker product. We will also consider the model reduction where we consider a smaller network consisting of 12 nodes, akin to case 2 for Steur's network. We can then compare both model reductions to see if clustering is still better at preserving the stability region for traveling wave solutions. By using the same method detailed in Section 5.1 we can vary our singular coupling strength and find the two points at which the traveling wave solution changes in stability. This yields the results in Table 5.1.

We see that the original network has a bigger stability region than both the clustered network and the smaller network consisting of half the number of nodes. This means that the clustered system cannot be used as an upper bound to approximate the original system, which was the case for the Steur's network. However, it still seems to have a bigger overlapping stability region with the original network than the smaller network. An interesting observation is that the stability region for the clustered network and the smaller network are more or less a half and a quarter of the size, respectively, of the stability region for the original network. Giving a reason as to why this is the case is difficult, since we do not know if this is merely a coincidence or a property of these type of simplifications. It is also difficult to compare the simplifications done for the ring structure to the simplifications considered in Steur's network, since in one case we cluster nodes where the vertices are undirected and in the other case vertices which are directed. Therefore, in the next section we will consider a modular network, so that there are more direct correlations to Steur's network.

5.2.3 Star-Shaped Network

To stay in theme, it would be interesting to look at another network consisting of a central ring structure and modules. Instead of considering a module where all of the nodes are connected with one another, we consider one where we have a series of nodes. This is a so-called star-shaped network, see Figure 5.8. We consider two coupling strengths σ and μ which denote the inter-modular and intra-modular coupling strengths respectively, exactly as in Steur's network.

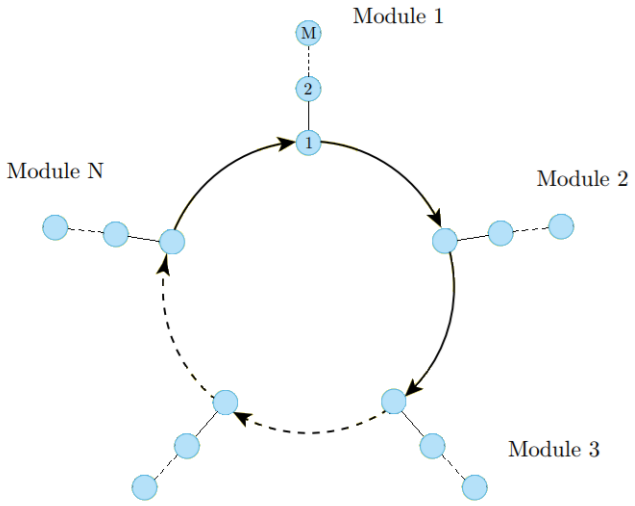

Figure 5.8: Star-shaped network consisting of N modules, each containing M nodes.

This allows us to vary both parameters to determine the curve of Neimark-Sacker bifurcations corresponding to a change in stability of the traveling wave solution. Next we have to choose how we simplify this network. We consider the following cases for a model reduction of the network

1. Clustering-based model reduction by clustering all but one of the nodes in each module.

2. Reduce the network size by lowering the number of nodes in each module to two.

3. Clustering-based model reduction by clustering the last two nodes in the series of each module.

The first two model reductions are exactly the same as the ones considered for Steur's network. We want to be able to compare these model reductions for different network structures, to see how this influences the preservation of the stability region of the original network.

We also want to see if clustering less nodes yields a better approximation of the original network. In case 3, we chose to cluster the final two nodes in each module. In other words, we will group node v_{M-1} with v_M and v_{2M-1} with

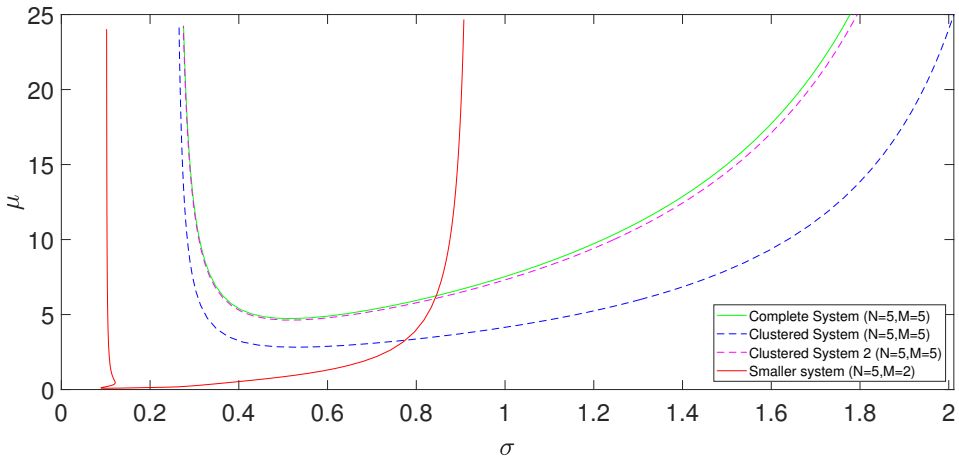

Figure 5.9: Stability regions for the ring network and for its model reductions considered in cases 1, 2 and 3. The parameter values are given in (2.2).

v_{2M}, etc. The resulting cluster matrix is given by

$$P = I_N \otimes \hat{P} = I_N \otimes \begin{bmatrix} 1 & 0 & \dots & 0 \\ 0 & 1 & \ddots & \vdots \\ \vdots & \ddots & \ddots & 0 \\ 0 & \dots & 0 & 1 \\ 0 & \dots & 0 & 1 \end{bmatrix}.$$

The clustering of an individual module is given by the matrix $\hat{P}$, which is extended to all of the modules with the help of the Kronecker product.

The stability regions for the original network and its model reductions are illustrated in Figure 5.9. The green curve corresponds to the stability region of the original network. The blue dashed and pink dashed curves correspond to the stability regions of the model reductions in cases 1 and 3, respectively. Lastly, the red curve corresponds to the stability region of the model reduction in case 2.

We will now discuss the results found for the so-called star-shaped network. The model reduction considered in case 1 preserves the stability region quite well, since it encompasses the stability region of the original network. However, this model reduction does not preserve the stability region as well as it did in Steur's network. If we look at the structure of the modules we can argue that this is due to the fact that the nodes are connected in a series instead of all being connected with one another. A more prevalent argument would be to look at how closely the oscillator solutions of the clustered nodes are grouped, see Figure 5.10. Notice how they are not as closely grouped as was observed in

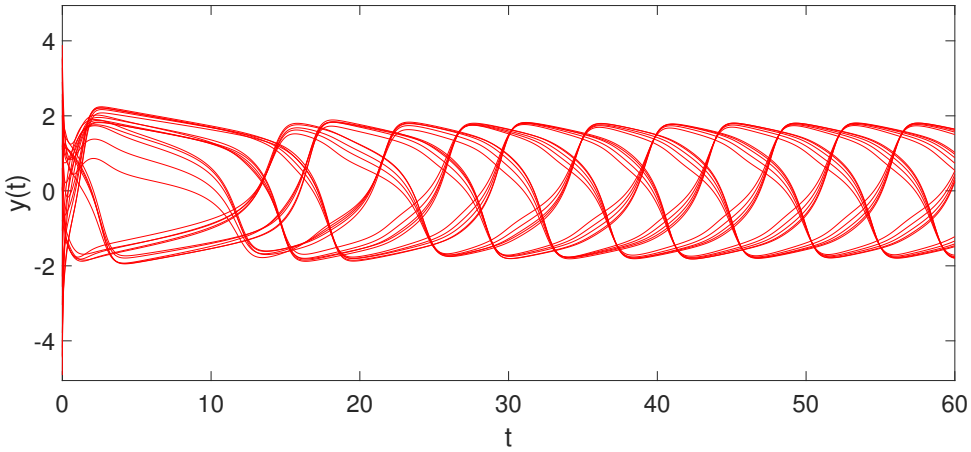

Figure 5.10: A traveling wave solution for the so-called star-shaped network ($N = 5$, $M = 5$). The parameter values are indicated in (2.2), with the coupling strengths $\sigma = 1$ and $\mu = 10$.

Steur's network. Some of the oscillator solutions in a module are more closely grouped than others. It turns out that the more grouped oscillator solutions correspond to the nodes at the end of the series in a module, and as we get closer to the node which constitutes to the ring structure, the solutions start to separate more. This would imply that clustering the nodes at the end of the series will yield a better approximation of the original system.

Case 2 actually yields the same network considered in case 2 of Steur's network. We can state again that the simplification in case 2 does not approximate the original network as well as the simplifications by clustering.

In case 3 we consider a different clustering in which we group the final two nodes in the module, these being the final two nodes in the series. We expected that clustering a smaller number of nodes would approximate the original network better than case 1. This is indeed the case, as the corresponding curve surrounds the curve of the original network a lot tighter. This is in line with what we speculated earlier. We can surmise that if we were to cluster two nodes in the middle of the series or at the start of the series that it would not be as good of an approximation as what we have considered in case 3.

These are all the cases we will consider in this thesis. In the next chapter we will draw some conclusions and give suggestions for future research.

Chapter 6

Conclusions

In this thesis we looked into applying a clustering-based model reduction on a network of nonlinear oscillators with the hopes of preserving specific dynamical behaviour. In particular, we looked at a network of FitzHugh-Nagumo oscillators. This network has the special property that it produces synchronized and traveling wave solutions for certain values of its coupling strengths. We considered three network structures, those being Steur's network, the ring network, and the star-shaped network. For these networks, we showed that applying a clustering-based model reduction is better at preserving the stability region for traveling wave solutions of the original network than simply reducing the network size. Furthermore, how well the clustering-based model reduction approximated the stability region of the original network depends on the interconnections of the clustered nodes and how close the oscillator solutions are for the clustered nodes. We also found that we need to take care when clustering, since it is possible to break one of the main structures of the network, resulting in a loss of preservation of the stability region.

Further research can be done with different types of network structures and especially by using different oscillators. It would be interesting to see if we would find the same results by using oscillators with different dynamics than the FitzHugh-Nagumo model. Due to long computation times with MatCont we could not consider larger network structures, which also limited the types of clusters we could consider. It would be interesting to see if the same results occur for larger network sizes, or see how they differ. However, the question is how we would select suitable clusters for the model reduction. From the main properties found, it seems we should start by looking at the solutions produced by the network. If we can pick nodes which have similar oscillators solutions, we would expect these to be a good choice for clusters. Before that, we can also look at the network structure. Groups of nodes with many connections between each other would also be good candidates for clusters.

Bibliography

[1] P. Blanchard, R. L. Devaney, and G. R. Hall, *Differential Equations*. Brooks/Cole, Cengage Learning, 2006.

[2] X. Cheng, "Model reduction of network systems with structure preservation: Graph clustering and balanced truncation," PhD thesis, University of Groningen, 2018.

[3] R. FitzHugh, "Impulses and physiological states in theoretical models of nerve membrane," *Biophysical Journal*, vol. 1, p. 447, 1961.

[4] Y. A. Kuznetsov, *Elements of Applied Bifurcation Theory*, second, ser. Applied Mathematical Sciences. Springer, 1998, vol. 112.

[5] M. Mesbahi and M. Egerstedt, *Graph Theoretic Methods in Multiagent Networks*. Princeton Series in Applied Mathematics, 2010.

[6] P. Mlinarić, S. Grundel, and P. Benner, "Clustering-based model order reduction for multi-agent systems with general linear time-invariant agents," *Max Planck Institute Magdeburg Preprints*, Jan. 2016.

[7] E. Steur *et al.*, "Coupling-modulated multi-stability and coherent dynamics in directed networks of heterogeneous nonlinear oscillators with modular topology," *IFAC-PapersOnLine*, pp. 062–067, 2016.

[8] E. Steur, "Synchronous behavior in networks of coupled systems : With applications to neuronal dynamics," DOI: 10.6100/IR718842, PhD thesis, Technische Universiteit Eindhoven, 2011.

[9] E. Steur *et al.*, "Directed cycles and multi-stability of coherent dynamics in systems of coupled nonlinear oscillators," *IFAC-PapersOnLine*, pp. 19–24, 2015.

[10] L. S. Tuckerman, "Maps, period doubling and Floquet theory," 2018.